

Combined-Cycle Gas Steam Turbine Power Plants

3rd Edition

**Rolf Kehlhofer
Bert Rukes
Frank Hannemann
Franz Stirnimann**

PennWell®

Contents

1. Introduction	1
2. The Electricity Market	5
3. Economics	11
4. Thermodynamic Principles of the Combined-Cycle Plant	35
5. Combined-Cycle Concepts	45
6. Applications of Combined Cycles	135
7. Components	165
8. Control and Automation	211
9. Operating and Part Load Behavior	225
10. Environmental Consideration	261
11. Developmental Trends	277
12. Integrated Gasification Combined Cycle	287
13. Carbon Dioxide Capture and Storage	321
14. Typical Combined-Cycle Plants	349
15. Conclusion	389
Appendix A: Conversions Table	393
Appendix B: Calculation of the Operating Performance of Combined-Cycle Installations	403
Appendix C: Symbols Used	405
Bibliography	407
Index	413
About the Authors	433

List of Figures

Figure 1–1	Simplified flow diagram of a combined cycle	2
Figure 2–1	Market development since 1975 of new power plants sold per year	9
Figure 3–1	Breakdown of the capital requirement for combined-cycle power plant	19
Figure 3–2	The cost of fuels over the years	23
Figure 3–3	Comparison of cost of electricity for base-load operation	29
Figure 3–4	Comparison of cost of electricity for intermediate load	30
Figure 3–5	Influence of fuel cost on the cost of electricity	31
Figure 3–6	Influence of the equivalent utilization time on the cost of electricity	32
Figure 3–7	Influence of interest rate on the cost of electricity	32
Figure 4–1	Temperature/entropy diagrams for various cycles	37
Figure 4–2	Gas turbine inlet temperature (TIT) definitions	38
Figure 4–3	The efficiency of a simple-cycle GT and a combined cycle plant as function of the gas turbine inlet temperature and pressure ratio	42
Figure 4–4a and 4–4b	The efficiency of a simple-cycle GT with single-stage combustion as a function of turbine inlet temperature (TIT) and turbine exhaust temperature	43
Figure 4–5a and 4–5b	The efficiency of a simple-cycle GT with sequential combustion as a function of the turbine inlet tempera- ture (TIT) and the turbine exhaust temperature	44
Figure 5–1	Selection of a combined-cycle power plant concept	46
Figure 5–2	Evolutionary change in combined-cycle design philosophy	47
Figure 5–3	Standardization approach	48
Figure 5–4	Entropy/temperature diagram for a gas turbine process at two different ambient air temperatures	52
Figure 5–5	Relative efficiency of gas turbine, steam process, and combined cycle as function of the air temperature	53
Figure 5–6	Relative power output of a gas turbine, steam turbine, and combined cycle as function of the air temperature	54

Figure 5–7	Relative power output of gas turbine, steam turbine, combined cycle, and relative air pressure versus elevation above sea level	55
Figure 5–8	Relative power output and efficiency of gas turbine and combined cycle as function of relative humidity . . .	56
Figure 5–9	Effect of water and steam injection on relative combined-cycle power	59
Figure 5–10	Effect of condenser pressure on steam turbine output . . .	62
Figure 5–11	Temperature of cooling medium versus condenser pressure for different types of cooling systems	63
Figure 5–12	Flow diagram to show fuel preheating	65
Figure 5–13	Steam turbine output and HRSG efficiency versus gas turbine exhaust temperature for a single-pressure cycle . . .	68
Figure 5–14	Ratio of steam turbine output of a dual pressure compared to a single-pressure cycle as a function of the gas turbine exhaust temperature	69
Figure 5–15	Energy/temperature diagram for an idealized heat exchanger	71
Figure 5–16	Flow diagram of a single-pressure cycle	73
Figure 5–17	Energy/temperature diagram of a single-pressure HRSG	75
Figure 5–18	Heat balance for a single-pressure cycle	76
Figure 5–19	Energy flow diagram for the single-pressure combined-cycle power	77
Figure 5–20	Effect of live steam pressure on steam turbine output for a single-pressure cycle (including steam turbine exhaust moisture content and HRSG efficiency)	78
Figure 5–21	Energy/temperature diagram of a single-pressure HRSG with live-steam pressure of 40 and 105 bar (566 and 1508 psig)	79
Figure 5–22	Effect of live-steam pressure on condenser waste heat at constant condenser pressure	80
Figure 5–23	Effect of live-steam temperature on steam turbine output for a single-pressure cycle with 105 bar (1508 psig) live-steam pressure (including HRSG efficiency and steam turbine exhaust moisture content) . . .	82
Figure 5–24	Effect of pinch point on relative steam turbine power output and relative HRSG heating surface	83

Figure 5–25	Influence of HRSG backpressure on combined-cycle output and efficiency, GT output and efficiency, and HRSG surface	85
Figure 5–26	Effect of feedwater temperature on steam turbine output and HRSG efficiency for cycles with one stage of preheating	87
Figure 5–27	Energy/temperature diagram for a single-pressure HRSG	88
Figure 5–28	Energy/temperature diagram for a conventional boiler	89
Figure 5–29	Flow diagram of a single-pressure cycle with LP preheating loop for high sulfur fuels	92
Figure 5–30	Flow diagram of a dual-pressure cycle for high sulfur fuel	93
Figure 5–31	Effect of feedwater temperature and number of preheating stages on steam turbine output of a dual-pressure cycle	94
Figure 5–32	Flow diagram of a dual-pressure cycle with low sulfur fuel	95
Figure 5–33	Heat balance for a dual-pressure cycle with low sulfur fuel	96
Figure 5–34	Energy flow diagram for a dual-pressure combined-cycle plant	97
Figure 5–35	Energy/temperature diagram for a dual-pressure HRSG	98
Figure 5–36	Effect of the HP and LP pressure on steam turbine output and exhaust moisture content for a dual-pressure cycle	101
Figure 5–37	Effect of LP pressure on HRSG efficiency for a dual-pressure cycle	102
Figure 5–38	Effect of HP and LP steam temperature on steam turbine output for a dual-pressure cycle	103
Figure 5–39	Effect of HP and LP pinch point on steam turbine output and relative HRSG surface for a dual-pressure cycle	104
Figure 5–40	Flow diagram of a triple-pressure cycle	106
Figure 5–41	Heat balance of a triple-pressure cycle	107

Figure 5–42	Energy/temperature diagram of a triple-pressure HRSG	108
Figure 5–43	Energy flow diagram of a triple-pressure combined-cycle plant	109
Figure 5–44	Steam turbine output and exhaust moisture content versus HP and IP pressure for triple-pressure cycles at constant LP pressure (5 bar)	110
Figure 5–45	Effect of LP pressure on steam turbine output and relative HRSG surface for triple-pressure cycles at constant HP (105 bar) and IP (25 bar)	111
Figure 5–46	Live-steam temperature optimization for a triple-pressure cycle	112
Figure 5–47	Temperature/entropy diagram showing the effect of “mild reheat” on the steam turbine expansion line	113
Figure 5–48	Effect of HP and IP evaporator pinch point on steam turbine output and relative HRSG surface for a triple-pressure cycle with constant LP pinch point	114
Figure 5–49	Flow diagram of a triple-pressure reheat cycle	116
Figure 5–50	Heat balance for a triple-pressure reheat cycle	117
Figure 5–51	Temperature/entropy diagram showing the effect of full reheat on the steam turbine expansion line	118
Figure 5–52	Energy flow diagram for a triple-pressure reheat combined-cycle plant	118
Figure 5–53	Energy/temperature diagram for a triple-pressure reheat HRSG	119
Figure 5–54	Steam turbine output and HRSG surface versus HP and reheat pressure for a triple-pressure reheat cycle at constant HP and reheat temperature (568/568°C)	120
Figure 5–55	Steam turbine output versus HP and reheat steam temperature for a triple-pressure reheat cycle at constant HP (120 bar), IP (30 bar) and LP (5 bar) pressure	122
Figure 5–56	Flow diagram of a high-pressure reheat cycle with a HP once-through HRSG and a drum-type LP section	123
Figure 5–57	Energy/temperature diagram for 647°C (A), 750°C (B) and 1000°C (C) exhaust gas temperature entering the HRSG	126

Figure 5–58	Effect of temperature after supplementary firing on power output and efficiency relative to that of a single-pressure cycle	127
Figure 5–59	Heat balance for a single-pressure cycle with supplementary firing	128
Figure 5–60	Performance of different combined cycles over the exhaust gas temperature	130
Figure 5–61	Influence of various parameters/measure on combined-cycle output and efficiency	132
Figure 5–62	Impact of HP and reheat steam parameters (pressure and temperature) on combined-cycle net efficiency	133
Figure 6–1	Simplified flow diagram of a cogeneration cycle with a back pressure turbine	137
Figure 6–2	Flow diagram of a cogeneration cycle with an extraction/condensing steam turbine	138
Figure 6–3	Flow diagram of a cogeneration cycle with no steam turbine	139
Figure 6–4	Heat balance for a single-pressure cogeneration cycle with supplementary firing	140
Figure 6–5	Effect of process steam pressure on relative combined-cycle power output and power coefficient for a single-pressure cycle with 750°C supplementary firing	142
Figure 6–6	Effect of power coefficient on electrical efficiency and fuel utilization for a single-pressure cycle with 750°C supplementary firing	143
Figure 6–7	Flow diagram of a cogeneration cycle with a dual-pressure HRSG	144
Figure 6–8	Comparison of 1-stage and 3-stage heating of district heating water	146
Figure 6–9	Heat balance for a cycle with two stages of district heating	147
Figure 6–10	Flow diagram of a district heating/condensing cycle	148
Figure 6–11	Flow diagram of a cycle coupled with a seawater desalination plant	150
Figure 6–12	Flow diagram of a conventional non-reheat steam power plant	152
Figure 6–13	Flow diagram of a combined-cycle plant using an existing steam turbine	152

Figure 6–14	Flow diagram of a gas turbine combined with a conventional steam cycle (fully fired combined-cycle plant)	155
Figure 6–15	Flow diagram of a parallel-fired combined-cycle plant	156
Figure 6–16	Flow diagram of a PFBC process	160
Figure 6–17	Flow diagram of a STIG cycle	161
Figure 6–18	Flow diagram of a turbo STIG cycle	162
Figure 6–19	Flow diagram of a HAT cycle	163
Figure 7–1	Turbine Inlet Temperature	167
Figure 7–2	Industrial Trent derived from the aero Trent 800	169
Figure 7–3	Heavy-duty industrial gas turbine	170
Figure 7–4	Gas turbine with sequential combustion	171
Figure 7–5	Types of losses contributing to overall performance degradation	175
Figure 7–6	Forced circulation heat recovery steam generator	184
Figure 7–7	Natural circulation heat recovery steam generator	185
Figure 7–8	Principle of drum-type and once-through evaporation	187
Figure 7–9	Three-pressure reheat once-through HRSG with drum-type LP and IP sections	188
Figure 7–10	Supplementary fired heat recovery steam generator	193
Figure 7–11	Different single-shaft combined-cycle configurations	197
Figure 7–12	Cross section of a 142 MW reheat steam turbine with a separate HP turbine and a combined IP/LP turbine with axial exhaust	199
Figure 7–13	Cross section of a two-casing steam turbine with geared HP turbine	200
Figure 7–14	Cutaway drawing of an air-cooled generator for use in combined-cycle power plants	202
Figure 7–15	Single-line diagram	203
Figure 7–16	Typical arrangement of an air-cooled condenser	204
Figure 7–17	Typical arrangement of a wet cell cooling tower	205
Figure 7–18	Principle of hybrid cooling tower	206
Figure 8–1	Hierarchic levels of automation	213
Figure 8–2	Standard layout for a modern combined-cycle power plant control room	214
Figure 8–3	Principle diagram for a combined-cycle load control system	216

Figure 8–4	Typical combined-cycle droop characteristic of a GT load controller	218
Figure 8–5	Closed control loops in a combined-cycle plant	219
Figure 9–1	Sliding pressure diagram	227
Figure 9–2	Effect of condenser vacuum on combined-cycle efficiency	231
Figure 9–3	Effect of frequency on relative combined-cycle output and efficiency for full-load operation	232
Figure 9–4	Effect of fuel composition and lower heating value on combined-cycle output and efficiency (base-load, gas-operation with wet cooling tower)	234
Figure 9–5	Part-load efficiency of gas turbine and combined cycle	235
Figure 9–6	Ratio of steam turbine and gas turbine output and live-steam data of a combined-cycle plant at part load	236
Figure 9–7	Part-load efficiency of combined-cycle plant with four single-shaft blocks	238
Figure 9–8	Performance guarantee comparison	241
Figure 9–9	Expected non-recoverable combined-cycle power plant degradation of power output and efficiency with GT operating on clean fuels	242
Figure 9–10	Gas turbine compressor efficiency as function of days operation (or operation hours)	243
Figure 9–11	Relative power increase of a combined-cycle power plant as function of ambient temperature and humidity	247
Figure 9–12	Typical arrangement of a fogging system in the GT air intake	248
Figure 9–13	Air inlet cooling process with chiller in Mollier diagram	250
Figure 9–14	Typical diagram of a chiller system	251
Figure 9–15	Startup curve for a 250–400 MW class combined cycle after eight hours standstill	256
Figure 9–16	Startup curve for a 250–400 MW class combined cycle after 48 hours standstill	257
Figure 9–17	Startup curve for a 250–400 MW class combined cycle after 120 hours standstill	257
Figure 9–18	Combined-cycle shutdown curve	258
Figure 9–19	Switch over diagram from gas to oil operation	259
Figure 10–1	NO _x equilibrium as a function of air temperature	263

Figure 10–2	Flame temperature as a function of the fuel-to-air ratio and combustion air conditions	264
Figure 10–3	NO _x concentration as a function of fuel-to-air ratio and combustion air conditions	265
Figure 10–4	NO _x reduction factor as a function of the water or steam-to-fuel ratio in gas turbines with diffusion combustion	266
Figure 10–5	Cross section of a low NO _x burner	269
Figure 10–6	Cross section of the Siemens dry low NO _x burner	270
Figure 10–7	Heat recovery steam generator with selective catalytic reduction	272
Figure 11–1	Chronology of the gas turbine inlet temperatures based on improved material and cooling technologies ..	279
Figure 11–2	Geared high-pressure turbine	283
Figure 11–3	Siemens SGT5-8000H gas turbine	284
Figure 11–4	Plant impact for fast cycling capability	285
Figure 12–1	Principle IGCC concept	287
Figure 12–2	Gasification reactions	288
Figure 12–3	Basic technologies of gasification and gasifier technology vendors	291
Figure 12–4	Entrained flow gasifiers	292
Figure 12–5	Schematic of Siemens full-water quench gasifier with water scrubbing	296
Figure 12–6	Schematic of shell coal gasification process with heat recovery and dry fly ash removal	297
Figure 12–7	Regenerable solvent-type AGR process	298
Figure 12–8	Claus process	299
Figure 12–9	Physical absorption process for simultaneous sulfur and CO ₂ removal	302
Figure 12–10	ASU process	303
Figure 12–11	Gas turbine syngas conditioning system (Siemens concept)	304
Figure 12–12	Effect of dilution and heating value on NO _x emission ..	305
Figure 12–13	Effect of dilution and heating value on NO _x emission ..	306
Figure 12–14	Gas turbine mass flow imbalance	307
Figure 12–15	IGCC concept based on hard coal and Shell gasification and Siemens combined-cycle technology	309
Figure 12–16	Sankey diagram of Shell-based IGCC concept	311

Figure 12–17	IGCC concept based on lignite and HTW gasification and Siemens combined cycle	312
Figure 12–18	IGCC concept with CO ₂ capture based on hard coal and Siemens fuel gasifier (SFG) and Siemens combined-cycle technology	314
Figure 12–19	IGCC concept with CO ₂ capture based on Shell gasification and Siemens combined-cycle technology	316
Figure 12–20	Sankey diagram of shell-based IGCC concept with CO ₂ capture	317
Figure 13–1	Historical trend of energy consumption and global warming	322
Figure 13–2	CO ₂ -emissions mitigating by fuel switch	323
Figure 13–3	Typical specific CO ₂ -emissions from fossil fuels	324
Figure 13–4	Typical trend of solubility in physical and chemical washing agents	326
Figure 13–5	Principle of ion transport membrane	328
Figure 13–6	Principle of chemical looping combustion	329
Figure 13–7	Schema of pre-combustion CO ₂ -capture	329
Figure 13–8	Combined autothermal reforming and CO ₂ -capture	332
Figure 13–9	Concept of an innovative premix burner for hydrogen-rich syngases	334
Figure 13–10	Schema of post-combustion CO ₂ -capture	335
Figure 13–11	Post-combustion absorption process	336
Figure 13–12	Post-combustion CO ₂ capture under pressure	338
Figure 13–13	Schema of Oxyfuel firing CO ₂ capture	339
Figure 13–14	Concept of the Graz cycle	340
Figure 13–15	Direct Oxyfuel fired CO ₂ capture, CES cycle	341
Figure 13–16	Principle of the AZEP process	342
Figure 13–17	Principle of the ZESOFc process	343
Figure 13–18	Expected CO ₂ avoidance and power generation costs for industrial-scale power plants in operation by 2020 (Source: ZEP)	345
Figure 14–1	View of Taranaki combined-cycle plant	350
Figure 14–2	Process diagram of Taranaki combined-cycle power plant	351
Figure 14–3	Arrangement of Taranaki combined-cycle power plant	353

Figure 14–4	Process diagram for Monterrey combined-cycle power plant	355
Figure 14–5	Layout of the Monterrey combined-cycle power plant	357
Figure 14–6	View of the Phu My 3 combined-cycle power plant	358
Figure 14–7	Process diagram of the Phu My 3 combined-cycle power plant	359
Figure 14–8	Arrangement of the combined-cycle reference power plant SCC5-4000F 2×1	359
Figure 14–9	View of the Palos de la Frontera combined-cycle power plant	361
Figure 14–10	Layout of the Palos de la Frontera combined-cycle power plant	362
Figure 14–11	Process diagram of the Palos de la Frontera combined-cycle power plant (one unit)	363
Figure 14–12	View of the Arcos combined-cycle power plant	365
Figure 14–13	View of Diemen combined-cycle cogeneration plant	368
Figure 14–14	Process diagram of Diemen combined-cycle cogeneration plant	369
Figure 14–15	General arrangement of Diemen combined-cycle cogeneration plant	371
Figure 14–16	View of the Shuweihat S1 plant	372
Figure 14–17	Process diagram of the Shuweihat S1 plant	373
Figure 14–18	Vado Ligure, old layout	375
Figure 14–19	Vado Ligure, new layout	377
Figure 14–20	Thermal process of repowered plant	380
Figure 14–21	CAD Image of the repowered plant	381
Figure 14–22	Flow scheme of Puertollano IGCC plant	382
Figure 14–23	Main technical data of the IGCC Puertollano	384
Figure 14–24	Availability between 1996 and 2003	384
Figure 14–25	Process diagram of the Monthel cogeneration power plant	386
Figure 14–26	Plant arrangement	386
Figure A–1	Calculation of operating and part-load behavior:	
	Method for solving the system of equations	402
	Conversion of the main units used in this book	403
	Conversion formulæ	403

List of Tables

Table 2–1	Installed capacity 2007	7
Table 2–2	World net electricity generation by type 2004 (TWh)	8
Table 2–3	World fuel consumption for fossil-fuelled power plants	8
Table 2–4	Fossil fuels: proved reserves vs. yearly consumption worldwide in 2007	10
Table 3–1	Specific price of various power plants in US\$/kW	19
Table 3–2	Net efficiency of various power plants	21
Table 3–3	Fuel flexibility of various power plants	22
Table 3–4	Variable operating and maintenance costs for various power plants of different sizes	24
Table 3–5	Fixed operation and maintenance costs for various power plants of different sizes	25
Table 3–6	Availability and reliability of various power plants	26
Table 3–7	Construction times for various power plants	28
Table 3–8	Inputs for economical comparison	29
Table 4–1	Thermodynamic comparison of gas turbine, steam turbine, and combined-cycle processes	36
Table 4–2	Allowable reduction in steam process efficiency as a function of gas turbine efficiency ($\eta_{ST} = 0.30$)	41
Table 5–1	Comparison of combined-cycle performance data for different cooling systems and ambient temperatures	61
Table 5–2	Possible fuels for combined-cycle applications	66
Table 5–3	Comparison multishaft versus single shaft	67
Table 5–4	Performance comparison of different cycle concepts (natural gas with low sulfur content and GT exhaust gas temperature of 647°C (1197°F))	129
Table 6–1	Conversion of a 500 MW steam turbine power plant into a parallel-fired combined-cycle plant	157
Table 7–1	Main characteristic data of modern gas turbines for power generation	171
Table 7–2	Critical fuel properties	176
Table 7–3	Typical composition of fuel gases for gas turbines	180

Table 7–4	Change of boundary conditions for steam turbines in combined-cycle plants	196
Table 8–1	Operation of steam turbine control loops in a single-shaft combined-cycle plant	222
Table 9–1	Overview of GT air inlet cooling systems	246
Table 9–2	Max ambient temperature and corresponding cooling potentials at different locations	246
Table 9–3	Typical example of combined cycle power improvement with chiller	252
Table 9–4	Specific investment costs for additional output of air inlet cooling system	253
Table 9–5	Expected startup times for a 400 MW combined-cycle plant	255
Table 10–1	Comparison of the heat to be dissipated for various types of 1,000 MW stations	274
Table 12–1	Emission of existing coal-based IGCC	289
Table 12–2	Commercial solid fuel IGCC plants 2007	290
Table 12–3	Allowed chemical impurities of gas turbine fuels (Siemens source)	295
Table 12–4	Investment and efficiency of IGCC concepts	313
Table 13–1	Typical hydrogen-enriched syngases downstream gas cleaning	332
Table 13–2	Characteristics of typical gas turbine fuels	333
Table 13–3	Commercially available CO ₂ absorption systems for post-combustion applications	337
Table 13–4	Selection of European CCS demonstration projects (source: The World Energy Book, issue 3)	347
Table 14–1	Combined-Cycle Plant examples—overview	349
Table 14–2	Main technical data of Taranaki combined-cycle power plant	352
Table 14–3	Main technical data of Monterrey combined-cycle power plant	356
Table 14–4	Main technical data of Phu My 3 combined-cycle power plant	360
Table 14–5	Main technical data of Palos de la Frontera combined-cycle power plant	364
Table 14–6	Main technical data of Arcos III combined-cycle power plant	367

Table 14–7	Main technical data of Diemen combined-cycle cogeneration plant	370
Table 14–8	Main technical data of the Shuweihat S1 Independent Water and Power Plant (IWPP)	374
Table 14–9	Main technical data of Vado Ligure combined-cycle power plant	378
Table 14–10	Main technical data of Monthel cogeneration plant	387

1

Introduction

This third edition of the book *Combined-Cycle Gas & Steam Turbine Power Plants* has been updated and extended to give an accurate picture of today's state of this interesting technology for power generation. It also includes chapters on actual themes such as CO₂ capture and storage, as well as integrated gasification combined-cycle plants (IGCC). These topics have gained a lot of attention as part of the discussion around global warming as potential solutions to this issue.

In substance, the book gives a comprehensive overview about the combined-cycle power plant from a thermodynamic, technical, and economical point of view. It is intended to provide material for lectures and provide an excellent understanding of the potential of this technology. Thanks to practical examples, it offers a real help for professional work. It is equally well suited for students interested in power generation.

The book strives to answer to the following two questions:

- What is a combined-cycle power plant?
- Why are combined-cycle plants among the leading technologies for large power plants?

Combined cycle can be defined as a combination of two thermal cycles in one plant. When two cycles are combined, the efficiency that can be achieved is higher than that of one cycle alone. Thermal cycles with

The risks remaining are mostly related to the plant itself: cost, efficiency and reliability.

The extreme case of this type of project is the **Tolling Agreement**. The investor has an agreement with a client, who supplies him with the fuel and takes off the electricity to convert the fuel into electricity at an agreed-upon fee, based on expected efficiency and availability.

The normal power plant project is, however, fully exposed to the market, which leads to a much higher risk profile. In this case, it is important to make a thorough market analysis in order to develop a solid market scenario. This analysis should include sensitivity analyses and worst-case scenarios.

In fossil fuel plants, both electricity and fuel markets have to be analyzed; however, both markets are coupled to a certain extent. For example, if in a given market most of the players are using gas as fuel, the price of electricity will go up if the gas prices are going up and vice versa.

The **interest and amortization cost** has a direct impact on the production cost of electricity produced. The main factors are:

- Debt-to-equity ratio
- Terms of the debt, such as interest and amortization

The debt-to-equity ratio depends mostly on the risk profile of the project. An IPP project with little market risk can be highly leveraged, which means a high percentage of the project financing can be provided in the form of debt. In good projects up to 80% of the capital required can be borrowed, and the equity share is only 20%.

In risky projects, a much lower leverage is possible. Typically, up to 50% of the capital required has to be provided as equity. The normal utility project falls in this category.

Normally, these merchant projects are realized by large utilities with a strong balance sheet. Financing is done based on the balance sheet of the investor (on-balance sheet financing). In this case, the borrower has the balance sheet of the owner of the power plant (the utility) as a guarantee.

So reliability is the percentage of the time between planned overhauls where the plant is generating or is ready to generate electricity, whereas the availability is the percentage of total time where power could be produced.

Availability and reliability have a big impact on plant economy. When a unit is down, power must be generated in another power station or purchased from another producer. In each case, replacement power is generally more expensive. The power station’s fixed costs are incurred whether the plant is running or not.

In deregulated markets, reliability is crucial. At peak tariff hours, a major portion of the income is generated and the plant must be reliable. Scheduled outages can be planned for off-peak periods when tariffs are close to or even below variable costs. Then only a small income loss results from the planned outages.

Typical average figures for the availability and reliability of well designed and maintained plants are indicated in table 3–6.

Table 3–6 Availability and reliability of various power plants

Type of Plant	Availability	Reliability
Combined cycle plant	90–94%	95–98%
Gas turbine plant (gas fired)	90–95%	97–99%
Steam turbine plant (coal fired)	88–92%	94–98%
Nuclear power plant	88–92%	94–98%

These figures are valid for plants operated at base load. They would be lower for peak- or intermediate-load operation because frequent startups and shutdowns reduce the lifetime of critical components and increase the scheduled maintenance and forced outage rates.

The major factors determining plant availability and reliability are:

- Design of the major components
- Engineering of the plant as whole, especially of the interfaces between the systems

considerations, it is generally better to burn the fuel directly in a modern gas turbine rather than in the HRSG because the temperature level at which heat is supplied to the process is higher (GT versus ST process in table 4–1). For that reason, the utilization of supplementary firing is decreasing.

The factors involved in combined-cycle installations with supplementary firing are discussed in more detailed in chapter 5.

Efficiency of combined cycles without supplementary firing in the HRSG

The most common and straightforward type of combined cycle is one in which fuel is supplied in the gas turbine combustion chamber without additional heat supplied in the HRSG. By substituting equations (4–4) and (4–7) into equation (4–2):

$$\begin{aligned}\eta_{CC} &= \frac{\eta_{GT}\dot{Q}_{GT} + \eta_{ST}\dot{Q}_{GT}(1 - \eta_{GT})}{\dot{Q}_{GT}} \\ &= \eta_{GT} + \eta_{ST}(1 - \eta_{GT})\end{aligned}\quad (4-8)$$

Differentiation makes it possible to estimate the effect that a change in efficiency of the gas turbine has on overall efficiency:

$$\frac{\partial \eta_{CC}}{\partial \eta_{GT}} = 1 + \frac{\partial \eta_{ST}}{\partial \eta_{GT}}(1 - \eta_{GT}) - \eta_{ST}\quad (4-9)$$

Increasing the gas turbine efficiency improves the overall efficiency only if:

$$\frac{\partial \eta_{CC}}{\partial \eta_{GT}} > 0\quad (4-10)$$

From equation (4–9):

$$-\frac{\partial \eta_{ST}}{\partial \eta_{GT}} < \frac{1 - \eta_{ST}}{1 - \eta_{GT}}\quad (4-11)$$

Improving the gas turbine efficiency is helpful only if it does not cause too great a drop in the efficiency of the steam process.

To ease the permitting process where water is not available, a direct air-cooling system with an air-cooled condenser (or a dry cooling tower as indirect system) is used. The disadvantages of this method include higher costs and higher exhaust steam (condenser) pressure, mainly in the off-design points with high ambient temperatures (therefore less power output of the steam turbine) leading to lower plant efficiency. In combined-cycle plants with a direct air-cooling system (ACC) the ambient air temperature directly influences the ST output and consequently the efficiency, which is not (or to a less extent) the case for the other cooling system (see table 5–1).

Table 5–1 Comparison of combined cycle performance data for different cooling systems and ambient temperatures

	Design: ambient temperature = 6°C (43°F)		Off-design: Summer ambient temp = 30°C (88°F)	
	P MW	Efficiency η %	P MW	η%
Cooling tower	411.7 100%	57.5 100%	363.5 100%	56.1 100%
ACC	408.1 99.1%	57.0 99.1%	345.4 95%	53.3 95%

In special cases where only a limited amount of water is available, and an evaporation system could be used with restrictions regarding visible plumes, a combination of a dry and wet system with hybrid cooler cells (consisting of a dry and a wet section) could be the optimal solution. Design parameters/performance data are similar to the wet cell cooling tower, but would result in slightly higher costs.

The temperature of the cooling medium has a major effect on the efficiency of the thermal process. The lower the temperature the higher the efficiency that can be attained, because the pressure in the condenser is lower, producing a greater useful enthalpy drop in the steam turbine and hence an increase in steam turbine output and in plant efficiency. This is illustrated in figure 5–10.

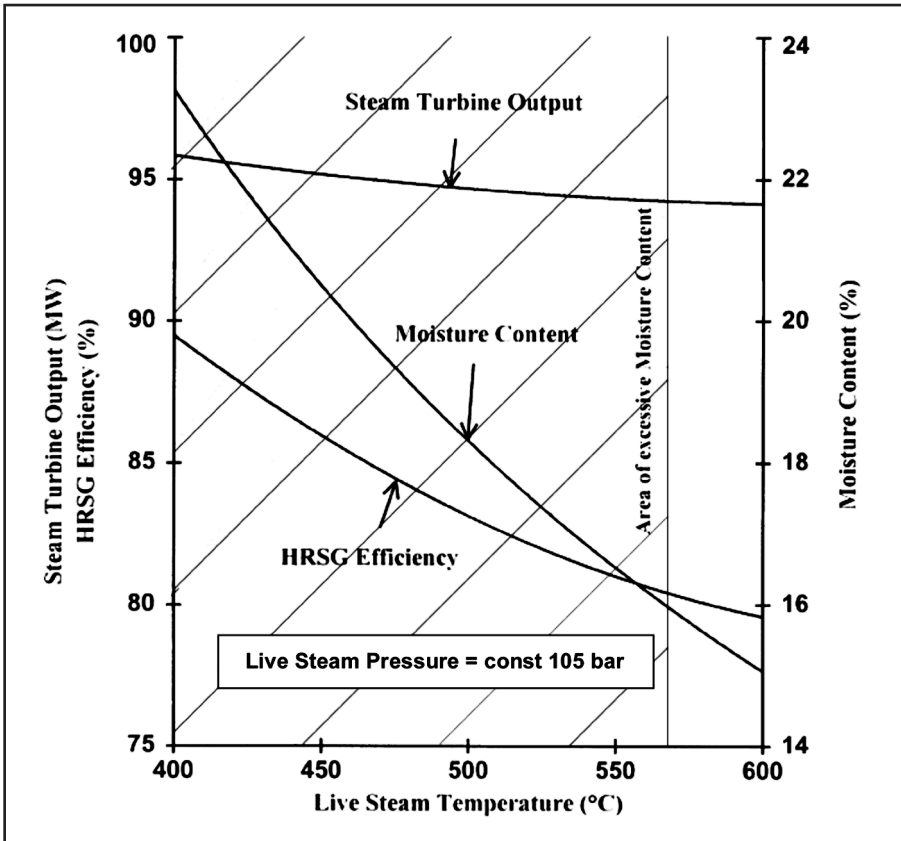


Figure 5-23 Effect of live-steam temperature on steam turbine output for a single-pressure cycle with 105 bar (1508 psig) live-steam pressure (including HRSG efficiency and steam turbine exhaust moisture content)

For gas turbines with lower exhaust gas temperatures than the one in the example, a lower live-steam pressure level would have to be chosen for the reasons previously discussed.